RSC Advances

PAPER

View Article Online
View Journal | View Issue

Cite this: *RSC Adv.*, 2019, **9**, 5288

Insights into the specific heat capacity enhancement of ternary carbonate nanofluids with SiO_2 nanoparticles: the effect of change in the composition ratio

Lixia Sang, * Wenming Ai, Tai Liu, Yuting Wu and Chongfang Ma

Received 16th December 2018
Accepted 26th January 2019

DOI: 10.1039/c8ra10318f

rsc.li/rsc-advances

Ternary carbonate nanofluids have proven to be a promising high temperature thermal energy storage and transfer medium for solar thermal power. For the ternary carbonate K_2CO_3–Li_2CO_3–Na_2CO_3 (4 : 4 : 2, mass ratio) with SiO_2 nanoparticles prepared using a two-step solution method, the enhancement of the specific heat capacity was up to 113.7% at 540 °C compared to the ternary carbonate prepared by a direct mixing method. The present work aims to give insights into the marked enhancement of specific heat capacity. The effect of evaporation temperature on the nanostructures formed in ternary carbonate nanofluids is discussed for the enhancement of specific heat capacity. More importantly, based on an analysis of inductively coupled plasma atomic emission spectrometry, it is revealed that the composition ratio of the ternary carbonate, which can influence its specific heat capacity, was changed during the evaporation process in an electrothermal drier. Besides a difference in the solubility of the carbonates in water, it is demonstrated that the heating mode can affect the composition ratio of mixed molten salts.

1. Introduction

Solar energy is regarded as the best renewable source to solve the problems of the energy crisis and environmental pollution, with the characteristics of being clean and inexhaustible.[1] Concentrated solar power (CSP) systems are promising technology for the collection and use of solar thermal energy to generate electricity.[2] Molten salts have been considered as good candidates for a thermal energy storage medium or a heat transfer fluid in CSP plants due to their higher operating temperature, better thermal stability and lower vapor pressure.[3,4] However, the main drawback of molten salts is their relatively poor specific heat capacity, which is generally less than 2 J g^{-1} K^{-1}.[5] If molten salts had a higher specific heat capacity, they could enable a significant improvement to heat transfer efficiency and reduce the cost of CSP plants.[6–8] Mixing molten salts with nanoparticles to form nanofluids is an effective approach to improving the specific heat capacity.[9–16]

Although nanoparticles in nanofluids can enhance the specific heat capacity, they aggregate easily and form clusters owing to their large specific surface area and high specific surface energy. Many experimental results have indicated that a good dispersion of nanoparticles in molten salts plays a significant role in enhancing the specific heat capacity.[17,18] To obtain molten salt nanofluids with better dispersion homogeneity, various nanoparticles with different sizes and concentrations have been widely applied and investigated.[19–24] Lasfargues *et al.*[22] obtained binary nitrate nanofluids by a mechanical dispersion method and found an increase of 10.48% in the specific heat capacity of a binary nitrate with 0.1 wt% CuO nanoparticles (29 nm). By mixing SiO_2 nanoparticles (60 nm) with a ternary nitrate using a two-step solution method, the enhancement of the specific heat capacity was 13% and the optimal concentration of SiO_2 was 1 wt%.[23] Through the two-step solution method, Shin *et al.*[24] prepared chloride salt eutectic nanofluids and found that the enhancement of the specific heat capacity was 14.5% when adding 1 wt% SiO_2 with a 26 nm diameter. As shown above, the two-step solution method has been used more in the preparation of molten salt nanofluids. In the second step, the sample solutions were evaporated by a hot plate in most studies.[17,18,23–27] Jo *et al.*[26] reported that the specific heat capacity of binary carbonate eutectic-carbon nanotube nanofluids increased linearly with the hotplate temperature. However, in Shin's study,[27] for Li_2CO_3–K_2CO_3 eutectic salt nanofluids with 1 wt% SiO_2 (10 nm), the average specific heat capacity of samples heated at 60 °C was higher than that of samples boiled at 100 °C. Explanation of the variation in the thermophysical properties of the different samples only referred to the amount of the agglomeration of the nanoparticles, as well as the formation of a compressed phase due to a different evaporation process. In fact, evaporation processes with different temperatures and heating modes may

Key Laboratory of Enhanced Heat Transfer and Energy Conservation of Ministry of Education, Key Laboratory of Heat Transfer and Energy Conservation Beijing Municipality, Department of Energy Science and Engineering, College of Environmental and Energy Engineering, Beijing University of Technology, Beijing 100124, China. E-mail: sanglixia@bjut.edu.cn

affect the composition ratio of molten salts. Differences in the composition ratio of mixed molten salts can bring about different specific heat capacities.[28] Therefore, more studies should focus on clarifying these factors for the enhancement of specific heat capacity of molten salt nanofluids.

In our previous work,[19] in order to improve the Rankine cycle efficiency of CSP, a ternary carbonate (TC) K_2CO_3–Li_2CO_3–Na_2CO_3 (4 : 4 : 2, mass ratio) with a relatively low melting point (410.5 °C) and a high decomposition temperature (over 800 °C) was selected as the base salts, and the specific heat capacity of the TC nanofluids with different nanoparticles (SiO_2, CuO, TiO_2, and Al_2O_3) or SiO_2 with different sizes were investigated. Among the chosen nanoparticles, SiO_2 nanoparticles proved to be the most effective additive in enhancing the specific heat capacity of the TC.[19] In the present work, we wanted to further explore the enhancement of the specific heat capacity of the TC nanofluids with SiO_2 nanoparticles. The TC nanofluids with SiO_2 nanoparticles were prepared using a two-step solution method. In the second step, the solutions of the samples were heated in an electrothermal drier rather than on a hot plate. The effects of the heating mode and the evaporation temperature on the specific heat capacity of the TC nanofluids were studied. Furthermore, the composition ratio changes of the as-prepared samples were analyzed, and their influence on the enhanced specific heat capacity was revealed.

2. Experimental

2.1. Preparation of the TC nanofluids

The TC was prepared by a direct mixing method. All carbonates were purchased from Tianjin Guangfu Technology Development Co. Ltd, with purities above 99.0%, and were used without further purification. SiO_2 nanoparticles were selected from Beijing DK Nanotechnology Co. Ltd. The average diameter of the SiO_2 nanoparticles, with a purity of 99.9%, was about 20 nm. The TC nanofluids with 1 wt% SiO_2 nanoparticles were prepared according to the steps in our previous work.[19] Firstly, 25 mg of SiO_2 nanoparticles were added to 250 mL deionized water, which was sonicated for 30 min. Then, 2.475 g ternary carbonate was dissolved in the water solution, and sonicated for 120 min to get a uniform solution. At last, the obtained mixed solution was evaporated in an electrothermal drier. Evaporation temperatures were set as 160, 180, 200 and 240 °C, and the corresponding samples were denoted as TC-SiO_2-160, TC-SiO_2-180, TC-SiO_2-200 and TC-SiO_2-240, respectively. In addition, the TC was also prepared using a two-step solution method with an evaporation temperature of 180 °C, in order to explore the effect of the preparation process on the property of the TC. The TC heated in an electrothermal drier was denoted as TC-180, and the TC heated on a hot plate was denoted as TC-180 P. All of the as-prepared samples are listed in Table 1.

2.2. Measurement of the specific heat capacity

The specific heat capacities of the pure TC and the TC nanofluids were analyzed based on the sapphire method using a Simultaneous Thermal Analyzer (STA-449F3, NETZSCH). According to the standard procedures of DIN51007, there should be a constant temperature at the beginning and the end of the procedure. Firstly, the temperature of the sample was heated at 40 °C for 15 min to ensure that the heat flux signal was stable. Secondly, the temperature of the sample was ramped to 580 °C at a fixed ramp rate of 10 °C min^{-1}. Lastly, the temperature of the sample was maintained at 580 °C for 15 min to reach a stable condition. The specific heat capacity of all of the samples was tested by the same procedure. Since the instrument may be not stable after turning it on, the first blank line with empty crucibles should be discarded. The sample used for the measurement, with a weight in the range of 10–15 mg, was dried at 140 °C for 2 h. In the sapphire method, the heat flows of an empty crucible, a crucible with sapphire and a crucible with the sample are measured in sequence. Then, the specific heat capacity of the sample is calculated by the three heat flow results and the specific heat capacity of sapphire. The specific heat capacity of all of the samples was measured three times to get the average value.

Uncertainties in the measurement are dependent on the measurement deviations for each of the parameters, including mass and heat flow. Taking f as a function of several independent parameters f_i, the n of the dependent parameter value is 2, and the measurement uncertainty can be determined by eqn (1):[14]

$$d(\ln f) = \sum_{i=1}^{n} \left| \frac{\partial \ln f}{\partial f_i} \right| \Delta f_i \quad (1)$$

The accuracy of the electronic balance was ±0.005 mg, and the accuracy of the heat flow was ±0.1 μW. Hence, the measurement uncertainty of the specific heat capacity was estimated to be less than 3% (relative).

2.3. Analysis of the microstructures and composition

The microstructures and EDS element mapping of the pure TC and the TC nanofluids were performed by scanning electron microscopy (SEM) (S-3400N, Hitachi). The surface areas of the

Table 1 The pure TC and the TC nanofluids prepared by a two-step solution method

Samples	Original constituents	Evaporation temperature
TC (ternary carbonates)	K_2CO_3–Li_2CO_3–Na_2CO_3 (4 : 4 : 2, mass ratio)	—
TC-SiO_2-160	K_2CO_3–Li_2CO_3–Na_2CO_3, 1 wt% SiO_2	160 °C
TC-SiO_2-180	K_2CO_3–Li_2CO_3–Na_2CO_3, 1 wt% SiO_2	180 °C
TC-SiO_2-200	K_2CO_3–Li_2CO_3–Na_2CO_3, 1 wt% SiO_2	200 °C
TC-SiO_2-240	K_2CO_3–Li_2CO_3–Na_2CO_3, 1 wt% SiO_2	240 °C
TC-180	K_2CO_3–Li_2CO_3–Na_2CO_3 (4 : 4 : 2, mass ratio)	180 °C (electrothermal drier)
TC-180 P	K_2CO_3–Li_2CO_3–Na_2CO_3 (4 : 4 : 2, mass ratio)	180 °C (hot plate)

nanofluids were analyzed using the Brunauer–Emmett–Teller (BET) method (TriStar II 3020, Micromeritics).

Inductively Coupled Plasma Atomic Emission Spectrometry (ICP-AES, 725E/Agilent) was used to measure the mass fraction of elements (Li, Na, K) in the as-prepared samples with a measurement uncertainty of less than 5% (relative). The measurement was repeated three times to get the average value. The composition ratio of the carbonates was calculated based on the average value of the mass fraction of the elements.

3. Results and discussions

3.1. Effects of the evaporation temperature on the specific heat capacity of the TC nanofluids

During the preparation, the evaporation temperature in the second step has a great influence on the dispersion of SiO_2 nanoparticles in the TC nanofluids.[18] Therefore, a suitable evaporation temperature would need to be selected, and so this was varied from 160 °C to 240 °C with temperature intervals of 20 °C during the preparation of the nanofluids. To confirm the accuracy of the instrument, the specific heat capacity of the binary carbonate Li_2CO_3–K_2CO_3 (62 : 38, molar ratio) was measured. The average value in the range of 525–555 °C was 1.59 J g^{-1} K^{-1}, which is close to the previously reported value in literature (1.60 J g^{-1} K^{-1}).[5] It is implied that this instrument and temperature program for the measurement of specific heat capacity is very reasonable. Fig. 1 shows the specific heat capacity curves of the TC nanofluids with SiO_2 nanoparticles prepared at different evaporation temperatures. For TC-SiO_2-160 and TC-SiO_2-180, there was a good repeatability of the specific heat capacity. However, the repeatability of the specific heat capacity results of TC-SiO_2-200 and TC-SiO_2-240 was poor.

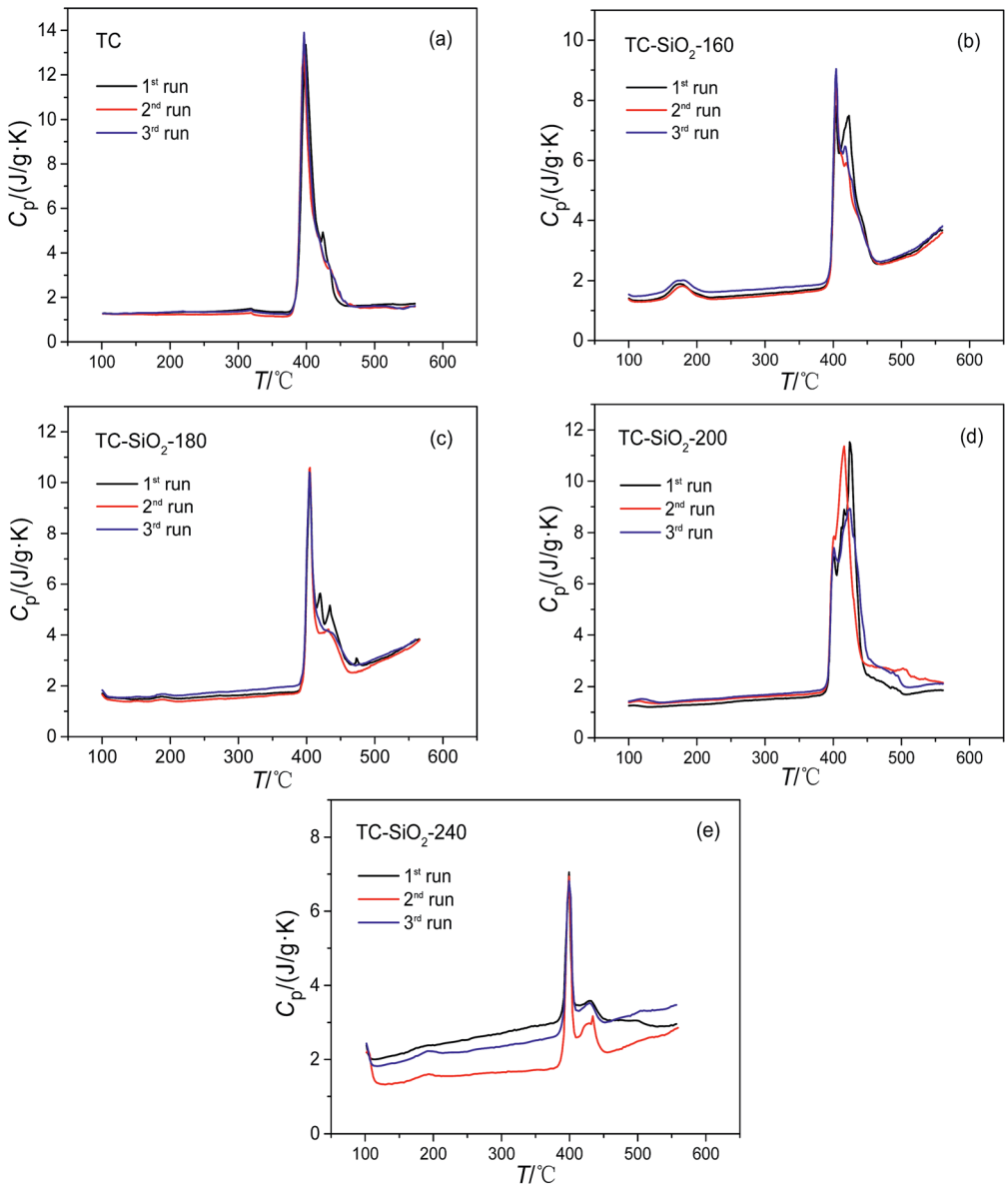

Fig. 1 Variation of specific heat capacity with temperature for the TC (a), and the TC nanofluids with SiO_2 nanoparticles prepared at an evaporation temperature of 160 °C (b), 180 °C (c), 200 °C (d), and 240 °C (e).

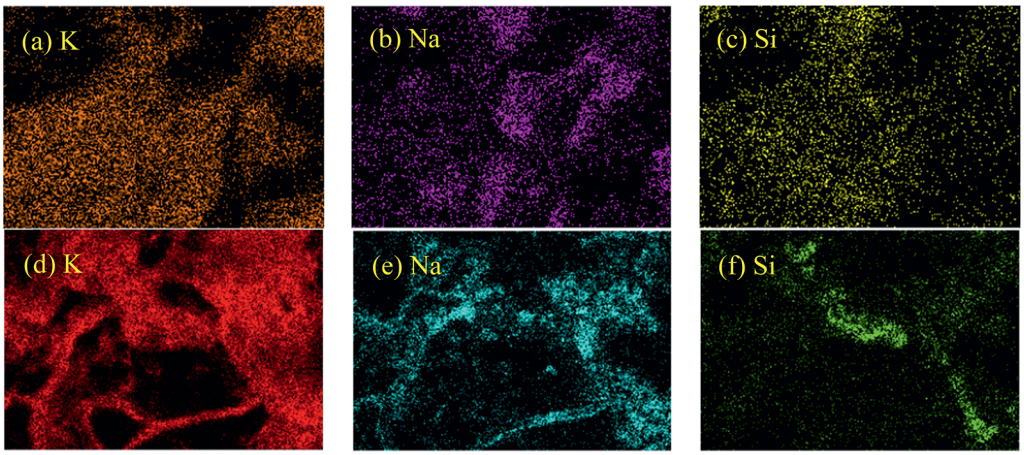

Fig. 2 EDS element mapping images of the TC-SiO_2-180 (a–c) and TC-SiO_2-240 (d–f).

During the evaporation process, a pool boiling phenomenon can be observed when the evaporation temperature is more than 200 °C. In particular, the pool boiling phenomenon was very evident at an evaporation temperature of 240 °C. In Shin *et al.*'s research,[29] they also mentioned that pool boiling can cause the degradation of specific heat capacity due to agglomeration of the nanoparticles. Furthermore, EDS element mapping of the nanofluids was performed to analyze the elemental distribution by scanning electron microscopy. As shown in Fig. 2, the elements Na, K and Si in TC-SiO_2-180 are distributed uniformly, which indicates that the nanoparticles can be effectively dispersed at an evaporation temperature of 180 °C. However, the elemental distribution at a evaporation temperature of 240 °C had significant agglomeration. Considering the dependence of the enhanced specific heat capacity on a homogeneous dispersion of the nanoparticles,[17] it is deduced that the pool boiling may cause the poor dispersion or agglomeration of SiO_2 nanoparticles in the TC.

Tables 2 and 3 show a comparison of the specific heat capacities of the pure TC and the TC nanofluids in the solid phase and in the liquid phase, respectively. As listed in Table 2, the specific heat capacities of TC-SiO_2-160, TC-SiO_2-180, and TC-SiO_2-200 in solid phase are greater than that of the pure TC. The enhancement of the specific heat capacity of TC-SiO_2-160 in the

Table 2 Comparison of specific heat capacities of the pure TC and the TC nanofluids with SiO_2 nanoparticles prepared at different evaporation temperatures in the solid phase

	Specific heat capacity, C_p (J g^{-1} K^{-1})		
Samples	320 °C	340 °C	360 °C
TC	1.37 (0.09)[a]	1.27 (0.09)[a]	1.25 (0.09)[a]
TC-SiO_2-160	1.64 (0.12)[a] (19.7)[b]	1.66 (0.11)[a] (30.7)[b]	1.71 (0.11)[a] (36.8)[b]
TC-SiO_2-180	1.70 (0.14)[a] (24.1)[b]	1.72 (0.15)[a] (35.4)[b]	1.78 (0.14)[a] (42.4)[b]
TC-SiO_2-200	1.63 (0.09)[a] (19.0)[b]	1.65 (0.10)[a] (30.0)[b]	1.69 (0.10)[a] (35.2)[b]

[a] The standard deviation of three measurements of the specific heat capacity. [b] The enhancement percentage of the specific heat capacity relative to the TC.

Table 3 Comparison of the specific heat capacities of the pure TC and the TC nanofluids with SiO_2 nanoparticles prepared at different evaporation temperatures in the liquid phase

	Specific heat capacity, C_p (J g^{-1} K^{-1})		
Samples	500 °C	520 °C	540 °C
TC	1.64 (0.08)[a]	1.65 (0.09)[a]	1.61 (0.09)[a]
TC-SiO_2-160	2.79 (0.07)[a] (70.1)[b]	2.98 (0.10)[a] (80.6)[b]	3.36 (0.04)[a] (108.7)[b]
TC-SiO_2-180	2.95 (0.10)[a] (79.9)[b]	3.17 (0.10)[a] (92.1)[b]	3.44 (0.08)[a] (113.7)[b]
TC-SiO_2-200	2.18 (0.43)[a] (32.9)[b]	2.03 (0.31)[a] (23.0)[b]	2.06 (0.21)[a] (28.0)[b]

[a] The standard deviation of three measurements of the specific heat capacity. [b] The enhancement percentage of the specific heat capacity relative to the TC.

solid phase is similar to that of TC-SiO_2-200, but both of them are less than that of TC-SiO_2-180. As shown in Table 3, the specific heat capacity of samples in the liquid phase increases more obviously, and the enhancement of the specific heat capacity of TC-SiO_2-160 and TC-SiO_2-180 is up to 70.1–108.7% and 79.9–113.7% in the range of 500–540 °C, respectively. Moreover, the enhancement of the specific heat capacity for liquid TC-SiO_2-180 is higher than that of liquid TC-SiO_2-160. This is because raising the evaporation temperature can shorten the evaporation time and reduce the agglomeration of nanoparticles in the nanofluids. However, when the evaporation temperature rises to 200 °C, the enhancement of the specific heat capacity of TC-SiO_2-200 decreases to be 23–32.9% in the range of 500–540 °C. The instability of TC-SiO_2-200 in liquid leads to a sharp increase in the standard deviation of three measurements of the specific heat capacity. Therefore, an evaporation temperature of 180 °C is more suitable to prepare the TC nanofluids with SiO_2 nanoparticles.

3.2. Understanding enhancement of the specific heat capacity of the TC nanofluids

Although study of the enhanced specific heat capacity of molten salt nanofluids has been a hot topic, a widely recognized mechanism has not been fully stated. As the specific heat capacity of SiO_2 nanoparticles (1.08 J g^{-1} K^{-1} at 334 °C (ref. 30)) is lower than that of the pure TC (1.65 J g^{-1} K^{-1} at 520 °C), adding nanoparticles into the TC would lead to a decrease in the specific heat capacity according to the thermal equilibrium model,[20] as follows:

$$C_{p,nf} = \frac{V_P \rho_p C_{p,p} + V_f \rho_f C_{p,f}}{V_p \rho_p + V_f \rho_f} \quad (2)$$

where C_p is specific heat capacity, V is volume fraction, ρ is density, and the subscripts nf, p, and f denote the property values of the nanofluid, nanoparticle, and base fluid. However, as shown in Section 3.1, the TC nanofluids with SiO_2 nanoparticles exhibit an enhanced specific heat capacity, which is opposite to the calculated results based on the thermal equilibrium model. There were no new substances produced in the TC nanofluids by X-ray diffraction (XRD), and there are no inflammatory reactions between the salts and SiO_2 nanoparticles.[19] This indicates that the enhancement of the specific heat capacity of the TC nanofluids needs to be analysed from the view of physics. Generally speaking, the specific heat capacity is directly related to the structure and phase of the material. Therefore, we firstly observed the change of the microstructure of the TC nanofluids by scanning electron micrography. Fig. 3 shows SEM images of the pure TC and the TC nanofluids prepared under different conditions.

It can be found from Fig. 3a that the surface of the pure TC is flat, and no special structure was formed. From Fig. 3e, the morphology of TC-SiO_2-240 was different from that of the TC, which may be the result of pool boiling. For TC-SiO_2-160, TC-SiO_2-180 and TC-SiO_2-200 shown in Fig. 3b–d, it can be found that needle-nanostructures are formed in these TC nanofluids with SiO_2 nanoparticles. In previous literature,[20] such special nanostructures were proposed to explain the enhancement of the specific heat capacity of molten salt nanofluids. Due to the OH^- on the surface of the SiO_2 nanoparticles, there is an electrostatic interaction between the nanoparticles and each compound of the mixtures, and then the salt mixtures are separated. The separated salt further crystallizes on the surface of the nanoparticles and forms nanostructures around these nanoparticles. These nanostructures have a very large specific

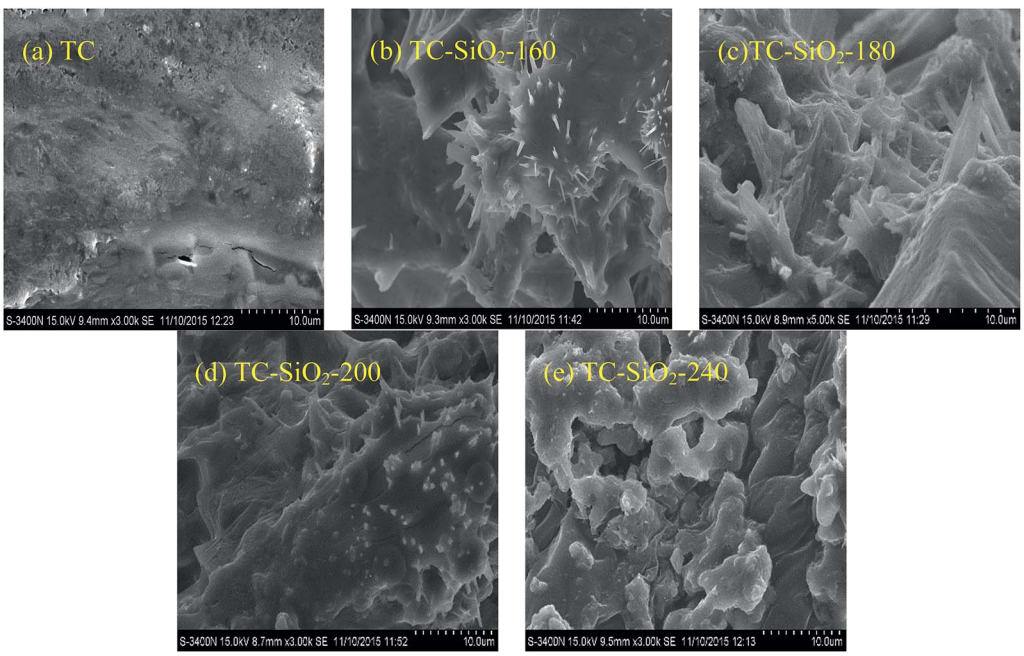

Fig. 3 SEM images of the pure TC (a) and the TC nanofluids: TC-SiO_2-160 (b), TC-SiO_2-180 (c), TC-SiO_2-200 (d), and TC-SiO_2-240 (e).

surface area and specific surface energy, which will contribute to enhancement of the specific heat capacity. As shown in Fig. 3b–d, only a few nanostructures are formed in TC-SiO_2-160 and TC-SiO_2-200, and more needle-like nanostructures can be found in TC-SiO_2-180. The surface areas of the TC, TC-SiO_2-160, TC-SiO_2-180, TC-SiO_2-200 and TC-SiO_2-240 are 24.38, 47.99, 49.48, 39.29 and 30.33 $m^2 g^{-1}$, respectively, which correspond to the number of nanostructures shown in the SEM images. The results showed that the surface area of the nanofluids can be increased by introducing SiO_2 nanoparticles with good dispersion. It may cause the enhancement of the specific heat capacity of TC-SiO_2-180 to be higher than that of TC-SiO_2-160 and TC-SiO_2-200 as shown in Tables 2 and 3. The significant nanoparticle agglomeration in the nanofluids prepared at an evaporation temperature of 240 °C results in a small surface area, which is not conducive to improvement of specific heat capacity. This may cause the enhancement of the specific heat capacity of TC-SiO_2-180 to be higher than that of TC-SiO_2-160 and TC-SiO_2-200 as shown in Tables 2 and 3. In Dudda *et al.*'s studies,[21] it was found that the specific heat capacity of binary nitrate nanofluids increased with increasing nanostructures.

More importantly, it is worthy to note that the enhancement of the specific heat capacity of the TC nanofluid with SiO_2 nanoparticles prepared at an evaporation temperature of 180 °C was up to 113.7% at 540 °C. Such a large enhancement of the specific heat capacity cannot be found in similar systems.[22–24] This cannot only be explained by the formation of nanostructures with a better dispersion of nanoparticles. It was reported that the composition ratio of the TC had a significant influence on their specific heat capacity.[28] Therefore, in order to explain the marked enhancement of the specific heat capacity, we analyzed the composition ratio of the ternary carbonate nanofluids by ICP-AES, and the results are shown in Table 4.

From Table 4, the composition of the molten salts in TC-180-SiO_2 is different from that of the TC prepared by the direct mixing method. Relative to the mass ratio of the preparation, the mass fraction of Li_2CO_3 in TC-180-SiO_2 was increased more than 32%. The specific heat capacity of ternary carbonates was more related to the mass fraction of Li_2CO_3.[28] A further question is how to bring about this big change in the mass fraction of Li_2CO_3. In the present work, the TC nanofluids with SiO_2 nanoparticles were prepared using the two-step solution method. On the one hand, the solubility of the TC in water is different, thus the salts can be crystallized in a different order in the evaporation process. Due to having the lowest solubility of the three carbonates (K_2CO_3–Li_2CO_3–Na_2CO_3), Li_2CO_3 can be formed first during evaporation. On the other hand, the sample solution was heated in an electrothermal drier in the second step, while the mixture solution was evaporated by a hot plate in most previous studies.[23,24] When heating by a hot plate, the mixed solution can be only heated from the bottom. Unlike the hot plate, the mixed solution in an electrothermal drier can be uniformly heated in all directions by hot air, which may be of benefit for the carbonates to separate out. To verify this, we also prepared TC-180 and TC-180 P using the solution method with an electrothermal drier and a hot plate, respectively. The composition ratios of TC-180 and TC-180 P were analyzed, and the results are shown in Table 4. It is obvious that the composition ratio of TC-180 P is similar to that of the TC, and the composition ratio of TC-180 is similar to that of TC-SiO_2-180, particularly the mass fraction of Li_2CO_3. The reason is clear for the big change in the composition ratio of the resultant samples. That is, this is caused by the heating mode in the evaporation process. Although the composition ratio of TC-180 is similar to that of TC-SiO_2-180, shown in Fig. 4, the specific capacity of TC-180 is lower than that of TC-SiO_2-180, which proves the role of the nanostructures based on nanoparticles on the specific capacity. Therefore, for TC-SiO_2-180 nanofluids, the changes in the composition ratio as well as the formation of nanostructures result in the marked enhancement of the specific heat capacity.

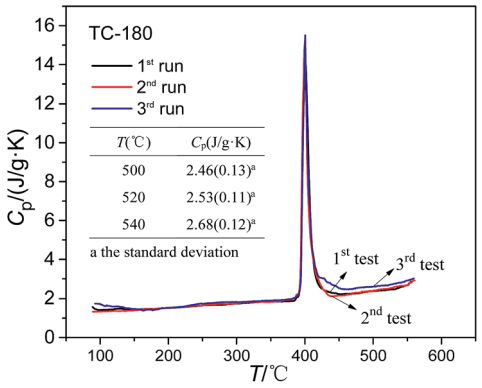

Fig. 4 Variation of the specific heat capacity with temperature for ternary carbonates (TC-180) prepared using the solution method with an electrothermal drier at an evaporation temperature of 180 °C.

Table 4 Comparison of the composition ratio of the pure TC and the TC nanofluids prepared at an evaporation temperature of 180 °C

	Mass ratio		
Samples	K_2CO_3	Li_2CO_3	Na_2CO_3
TC	0.40 (22.80)[a]	0.39 (7.37)[a]	0.21 (9.26)[a]
TC-180-SiO_2	0.24 (13.49)[a]	0.71 (13.44)[a]	0.11 (4.76)[a]
TC-180	0.19 (10.86)[a]	0.73 (13.84)[a]	0.14 (6.06)[a]
TC-180 P	0.41 (22.90)[a]	0.38 (7.28)[a]	0.22 (9.57)[a]

[a] Numbers in brackets show the average mass fractions of K, Li or Na in samples measured by ICP-AES.

4. Conclusions

In this study, nanofluids of ternary carbonates K_2CO_3–Li_2CO_3–Na_2CO_3 (4 : 4 : 2, mass ratio) with 1 wt% SiO_2 nanoparticles were prepared using a two-step solution method with different evaporation temperatures (160, 180, 200 and 240 °C). When evaporating at 180 °C in an electrothermal drier, the enhancement of the specific heat capacity of TC-180-SiO_2 was up to 79.9–113.7% in the range of 500–540 °C, compared to the TC prepared by a direct mixing method. On the one hand, the evaporation temperature plays an important role on the

formation of nanostructures in nanofluids. On the other hand, the marked enhancement of the specific heat capacity can also be attributed to the changes in composition, particularly the mass fraction of Li_2CO_3. The composition of the molten salts in TC-180-SiO_2 is different from that of the TC prepared by the direct mixing method. The different heating modes in the evaporation process, *i.e.* a hot plate and an electrothermal drier, can also lead to the big change in the composition ratio of the resultant samples. The present work reveals the effects of the preparation method on the composition ratio of the TC nanofluids, which will provide important information for developing TC nanofluids for application in CSP systems.

Conflicts of interest

There are no conflicts to declare.

Acknowledgements

The authors gratefully acknowledge the financial support of the National Key R&D Program of China (No. 2016YFE0124900) and the Research Program of the Beijing Natural Science Foundation (No. 3151001).

References

1 N. Zhang, B. Wang and Z. Liu, *Energy*, 2016, **99**, 10–19.
2 H. L. Zhang, H. Benoit, I. Perez-Lopèz, G. Flamant, T. W. Tan and J. Baeyens, *Renewable Energy*, 2017, **111**, 438–446.
3 D. Kearney, U. Herrmann, P. Nava, B. Kelly, R. Mahoney, J. Pacheco, R. Cable, N. Potrovitza, D. Blake and H. Price, *J. Sol. Energy Eng.*, 2003, **125**, 293–299.
4 Y. Wu, J. Li, M. Wang, H. Wang, Y. Zhong, Y. Zhao, M. Wei and Y. Li, *RSC Adv.*, 2018, **8**, 19251–19260.
5 N. Araki, M. Matsuura, A. Makino, T. Hirata and Y. Kato, *Int. J. Thermophys.*, 1988, **9**, 1071–1080.
6 M. H. Kim, H. Kim, R. K. Dong and K. S. Lee, *Energy Convers. Manage.*, 2016, **110**, 494–500.
7 S. Turrini, M. Bettonte, M. Eccher, M. Eccher, M. Grigiante and A. Miotello, *Renewable Energy*, 2018, **123**, 150–161.
8 P. Javadian, D. A. Sheppard, T. R. Jensen and C. E. Buckley, *RSC Adv.*, 2016, **6**, 94927–94933.
9 S. U. S. Choi and J. A. Eastman, *Proceedings of International Mechanical Engineering Congress and Exhibition*, USA, 1995, pp. 99–105.
10 S. U. S. Choi, Z. G. Zhang, W. Yu, F. E. Lockwood and E. A. Grulke, *Appl. Phys. Lett.*, 2001, **79**, 2252–2254.
11 S. M. S. Murshed, K. C. Leong and C. Yang, *Int. J. Therm. Sci.*, 2005, **44**, 367–373.
12 J. A. Eastman, S. U. S. Choi, S. Li, W. Yu and L. J. Thompson, *Appl. Phys. Lett.*, 2001, **78**, 718–720.
13 F. Yavari, H. R. Fard, K. Pashayi, M. A. Rafiee, A. Zamiri, Z. Z. Yu, R. Ozisik, T. B. Tasciuc and N. Koratkar, *J. Phys. Chem. C*, 2011, **115**, 8753–8758.
14 S. Harikrishnan, S. Magesh and S. Kalaiselvam, *Thermochim. Acta*, 2013, **565**, 137–145.
15 J. Seo and D. Shin, *Appl. Therm. Eng.*, 2016, **102**, 144–148.
16 M. X. Ho and C. Pan, *Int. J. Heat Mass Transfer*, 2014, **70**, 174–184.
17 M. Chieruzzi, A. Miliozzi, T. Crescenzi, L. Torre and J. M. Kenny, *Nanoscale Res. Lett.*, 2015, **10**, 273–282.
18 B. Jo and D. Banerjee, *Acta Mater.*, 2014, **75**, 80–91.
19 L. X. Sang and T. Liu, *Sol. Energy Mater. Sol. Cells*, 2017, **169**, 297–303.
20 H. Tiznobaik and D. Shin, *Int. J. Heat Mass Transfer*, 2013, **57**, 542–548.
21 B. Dudda and D. Shin, *Int. J. Therm. Sci.*, 2013, **69**, 37–42.
22 M. Lasfargues, Q. Geng, H. Gao and Y. L. Ding, *Nanomaterials*, 2015, **5**, 1136–1146.
23 J. Seo and D. Shin, *Micro Nano Lett.*, 2014, **9**, 817–820.
24 D. Shin and D. Banerjee, *Int. J. Heat Mass Transfer*, 2011, **54**, 1064–1070.
25 B. Jo and D. Banerjee, *J. Sol. Energy Eng.*, 2015, **137**, 1–9.
26 B. Jo and D. Banerjee, *International Conference on Energy Sustainability*, USA, 2010, pp. 741–748.
27 D. Shin and D. Banerjee, *Int. J. Struct. Changes Solids*, 2010, **2**, 25–31.
28 B. Jo and D. Banerjee, *J. Renewable Sustainable Energy*, 2015, **7**, 109–124.
29 D. Shin and D. Banerjee, *Int. J. Heat Mass Transfer*, 2014, **74**, 210–214.
30 C. W. Bale, P. Chartrand, S. A. Degterov, G. Eriksson, K. Hack, R. B. Mahfoud, J. Melancon, A. D. Pelton and S. Petersen, *Calphad*, 2002, **33**, 295–311.

